

**MAPPING PARTICLE PRECIPITATION ON TETHYS' SURFACE TO UNDERSTAND SPACE WEATHERING OF ITS ICY REGOLITH.** D. Schriver<sup>1</sup>, X. Jia<sup>2</sup>, and D. Domingue<sup>3</sup>, <sup>1</sup>UCLA, 3871 Slichter Hall, Los Angeles, CA 90095-1567, dschrive@ucla.edu, <sup>2</sup>University of Michigan, Ann Arbor, MI, xzjia@umich.edu, <sup>3</sup>Planetary Science Institute, 1700 E. Fort Lowell, Tucson AZ 85719, domingue@psi.edu

**Introduction:** The mineral composition of a satellite's surface informs our understanding of its origin, formation, and geologic evolution. Mineral composition is determined from remote sensing observations, namely spectral and color imaging observations. However, exogenic processes such as radiation from magnetospheric or solar wind particles alter the chemical and physical properties, thus affecting spectral and color imaging observations. The goal of this study is to map the precipitation of magnetospheric particles onto Tethys' surface, the first step in examining the correlation between surface radiation and color/spectral properties.

**Tethys' Space Environment:** Tethys, which has a radius of 531 km, has an orbital distance of about 5  $R_S$  ( $R_S$  = Saturn's mean radius  $\sim 60,268$  km), placing the moon within the inner part of the Saturnian magnetosphere, where the magnetic field is strongly dipolar. In this region, Tethys is exposed primarily to the dense, cool plasma that originates from the moon Enceladus, which is the main source of neutrals and plasma for Saturn's magnetosphere. The Enceladus plasma torus (with ions up to the keV energy range) is mainly composed of the water-group ions with minor contributions from  $H^+$  and  $H_2^+$  [1]. In addition to the cold plasma, energetic particles (keV to MeV protons and electrons) are also present at the orbits of the innermost moons [2].

At Tethys' orbit, the ambient magnetospheric plasma approximately co-rotates with the planet at bulk flow speeds larger than the Keplerian speed of the satellite's orbital motion. Therefore, Saturn's co-rotating plasma continually overtakes Tethys from its trailing side, resulting in a plasma wake on the leading side. For energetic particles, because they undergo gradient and curvature drift, in addition to gyromotion around the magnetic field, their trajectories relative to Tethys can vary significantly from convective co-rotation flow streamlines.

**Methodology:** To determine the precipitation energy and flux profile at Tethys due to the complicated interplay between particle flow speed and energy, and the external magnetic and electric field configuration, global kinetic numerical simulations are employed that follow charged particle motion in the large-scale electric and magnetic fields of Saturn. Here a global magnetohydrodynamic (MHD) simulation of Tethys' plasma interaction with Saturn's magnetosphere is used, which produces a reasonable representation of the

electric and magnetic field configuration around Tethys, along with large scale kinetic (LSK) particle tracing simulations to create precipitation maps at Tethys.

**Results:** Figure 1 shows MHD simulation results of the interaction of the Saturnian plasma with Tethys.

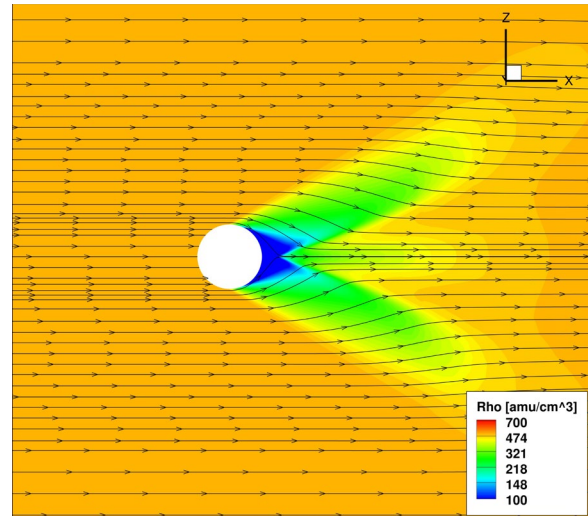


*Figure 1. Plasma density contours are color-coded with orange-red showing the highest (ambient) densities and blue showing lower densities. The black lines show plasma flow streamlines, flowing from left to right. Tethys is shown by the white circle with the vertical Z axis along the north-south geographic direction (north up, south down) and the horizontal X axis along the orbital motion direction with the leading hemisphere of Tethys to the right and the trailing hemisphere at left.*

From an MHD standpoint, which treats the magnetospheric plasma as a single magnetized fluid, precipitation onto the surface is primarily due to direct impact of the convecting, co-rotating plasma that overtakes the moon onto the surface of Tethys on the trailing hemisphere side (at left of white circle in figure 1), while a density cavity forms on the leading hemisphere side with very little precipitation occurring.

When kinetic (non-fluid) effects are considered, the precipitation profile differs from the fluid picture, with particle energy and pitch angle a primary factor influencing the precipitation location. To quantify the kinetic effects, LSK simulations are used whereby up to a million individual ion and electron particle trajectories are followed in the MHD magnetic and electric fields

around Tethys. The precipitation profile onto Tethys for a 50 eV Maxwellian distribution of protons is shown in figure 2.

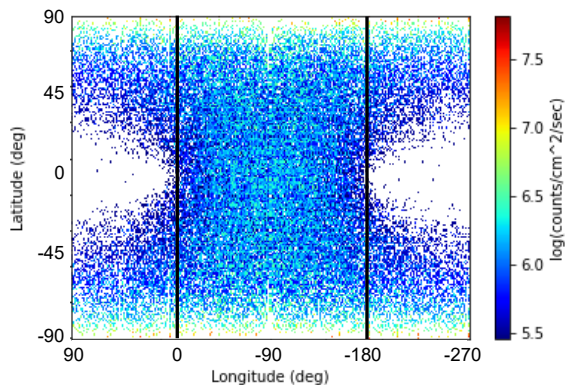


*Figure 2. Latitude versus longitude precipitating particle flux color contours are shown on a log scale. On the vertical axis, the geographic equator is at  $0^\circ$  latitude,  $\pm 90^\circ$  latitude corresponds to the North/South Pole. The horizontal geological longitude axis is centered on the trailing hemisphere ( $-90^\circ$ ), with  $0^\circ$  longitude corresponding to the hemisphere facing Saturn and  $+90^\circ/-270^\circ$  facing the leading hemisphere.*

Although much of the particle precipitation impact is on the trailing hemisphere of Tethys, which corresponds to the plasma flow facing side bounded by the solid vertical lines in figure 2, there is significant precipitation on the leading side of the moon particularly at higher latitudes. This is due to finite gyro-radius motion of charged particles in Saturn's magnetic field, as well as free motion of charged particles parallel to the ambient magnetic field. As the particle energy increases, the charged particle kinetic-effect precipitation is greatly enhanced resulting in significant precipitation on nearly all sides of the moon, which is quite different from the fluid picture. Results will be presented for all plasma species (water-group ions, protons and electrons) over a wide energy range.

**Acknowledgments:** This work was funded under NASA's Cassini Data Analysis Program grant 80NSSC20K0382.

**References:** [1] Thomsen, M.F., et al. (2010) *JGR* 115, A10220. [2] Kollmann, P., et al. (2011), *JGR*, 116, A02217.